2.8 ASTRAL 3-CONFIGURATIONS WITH DIHEDRAL SYMMETRY GROUP

In contrast to the chiral astral configurations that — in a certain sense — are all formed alike, the dihedral ones come in several very different varieties.

The first variety consists of configurations that are astral in the **e**xtended **E**uclidean plane but are not contained in the Euclidean plane itself; we shall refer to them as EE configurations. It is clear that such configurations must have one orbit of points at infinity, hence the other orbit of points needs to consist of the vertices of an isogonal polygon. In fact, the polygon must be regular. Indeed, consider any point at infinity and the three lines incident with it, hence mutually parallel. Since there are only two transitivity classes of lines, two of these lines must be in the same orbit; this implies that the third line is situated between these two, and is in fact a mirror interchanging the two lines. Therefore the sides of the polygon contained in these lines are congruent, that is, the pairs of points are at equal distance apart. But since each vertex must be on a third line (besides the two determined by the sides of the isogonal polygon), that line must be a mirror as well and therefore the adjacent sides of the polygon are of equal length. Hence the polygon is regular, and the configuration can be described as follows:

Theorem 2.8.1. If C is an (n_3) configuration of type EE, hence with dihedral symmetry group, that is astral in the extended Euclidean plane but is not contained in the Euclidean plane itself, then $n = 3m$ for some $m \geq 3$. The points of C are of the vertices of a regular $(2m)$-gon M and the m points at infinity in the directions of the m longest diagonals of M. The lines of C are the ones determined by the m longest diagonals of M, together with the $2m$ lines determined by pairs of points of M at span $m - j$ for some $0 < j < m/2$ with $j \equiv m \pmod 2$. The symmetry group of C is d_{2m}.

The EE configurations can therefore be characterized by a pair of integers m and j, and denoted by $EE(3m;m,j)$, with $0 < 2j < m \geq 3$ and with $j \equiv m \pmod 2$. Several examples of EE configurations are shown in Figure 2.8.1.

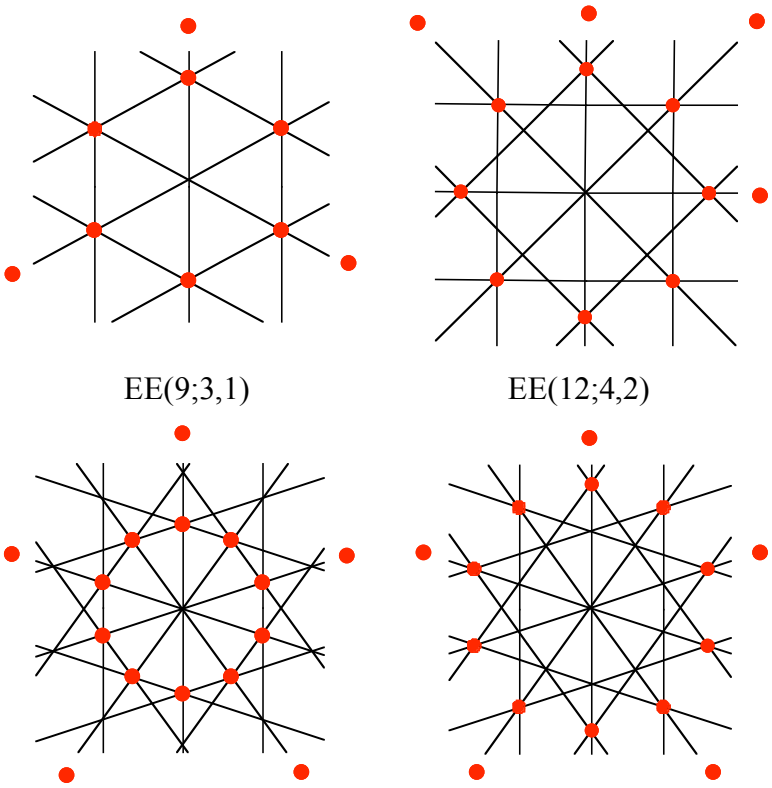

Figure 2.8.1. Examples of configurations of type EE. In each case, points at infinity in the directions of the longest diagonals are indicated by the detached dots.

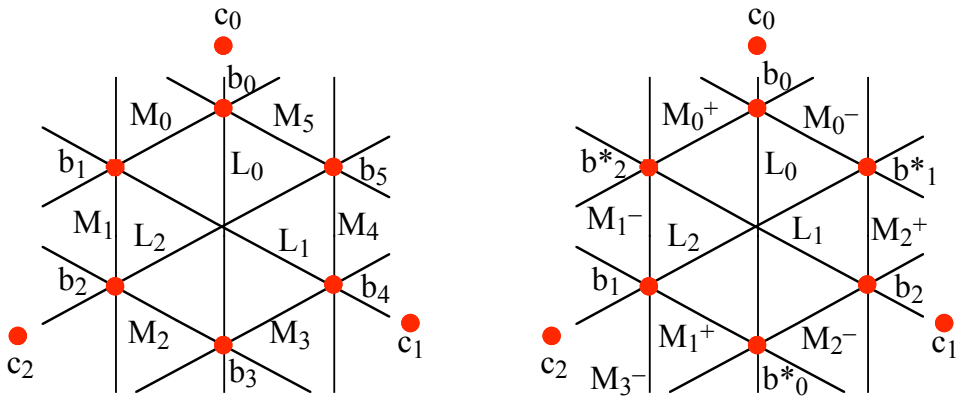

Figure 2.8.2. The configuration EE(9;3,1) labeled with the symmetry group c_6 (at left) and d_6 (at right). In both cases, the c points and the L lines are mapped onto themselves by halfturns.

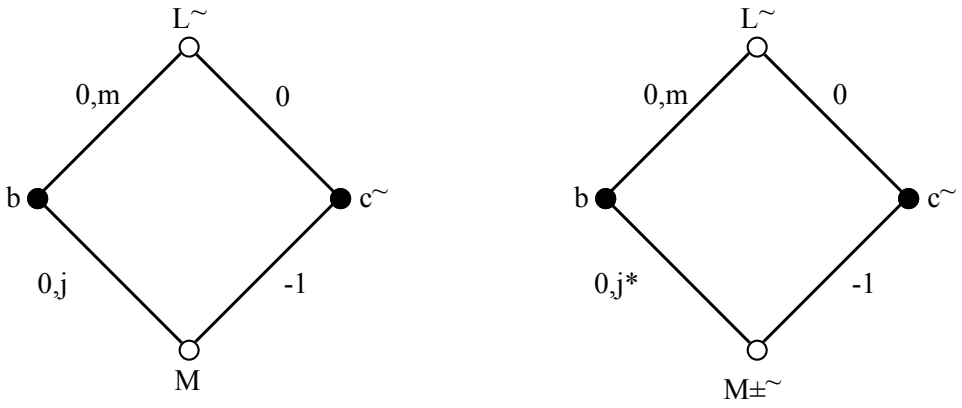

Symmetry group c_{2m} Symmetry group d_{2m}

Figure 2.8.3. The reduced Levi graphs of configurations EE(3m;m,j). All labels are understood mod 2m.

The second variety of dihedral astral 3-configurations may be thought of as **d**ihedrally **d**oubled-up chiral astral configurations, and we shall call them DD configurations. The typical notation is m#(b,c;d;μ); it will be explained soon. The DD configurations resemble chiral astral configurations in many respects, but there is one large difference.

First, the difference. The construction of chiral astral configurations starts with a set of points at the vertices of a **regular** polygon. In the dihedral case, the 2m vertices of any **isogonal** polygon can serve as starting points of a DD configuration ($(4m)_3$). Such vertices fall into two subsets of equal size, the m points in each subset being related by rotational symmetries of the whole set. The two subsets of points are images of each other under reflective symmetries of the whole set. The last entry μ in the symbol m#(b, c; d; μ) of a dihedral astral (n_3) configuration of type DD refers to the ratio (not exceeding 1) of the angles subtended by the sides of the isogonal (2m)-gon used in the construction.

Next, the similarities. There are again — naturally, in view of the definition of astrality — two orbits of points and two orbits of lines. Due to the presence of reflections, each orbit of elements has two suborbits, each suborbit consisting of m elements that are equivalent under rotations, without the need for reflections. In the example shown in Figure 2.8.4, and in general, the points in the two suborbits of the first class are

denoted by B_j^+ and B_j^-, those in the second class by C_j^+ and C_j^-. If $b \neq c$, we shall usually assume $b > c$. The points B_j^+ and B_j^- are on endpoints of diagonals of span b of each of the two m-gons determined by points of the suborbit, while C_j^+ and C_j^- are on diagonals of span c of the other two m-gons. One of the mirrors is the bisector of $B_0^+B_0^-$; it is indicated in Figure 2.8.4 by the dashed vertical line. The B_j^+ and B_j^- points are obtained by rotation in counterclockwise orientation. The construction of the configuration m#(b, c; d; μ) proceeds as follows; it is illustrated in Figure 2.8.4, where $m = 5$, $b = 2$, $c = 1$, $d = 1$, and $\mu = 0.6$.

B_0^+ and B_b^+ determine the line L_0^+ and the point C_0^+, which divides the segment $B_0^+B_b^+$ in a ratio λ; this ratio is fixed throughout the construction, but still undetermined. More generally, B_j^+ and B_{j+b}^+ determine C_j, clearly with the same ratio λ. Then the line M_0^+ in determined by C_0^+ and C_c^+; it passes through B_d^-, and more generally, C_j^+ and C_{j+c}^+ determine the line M_j^+ that is incident with B_{j+d}^-. This requirement determines the value of λ through a quadratic equation. In turn, the line L_d^- through B_d^- and B_{d-b}^- passes through C_d, and finally C_d^- and C_{d-c}^- are collinear with B_0 on the line M_d^-. As always, the subscripts are understood to be modulo m. These requirements can all be met simultaneously, due to the symmetry of the sets of points involved.

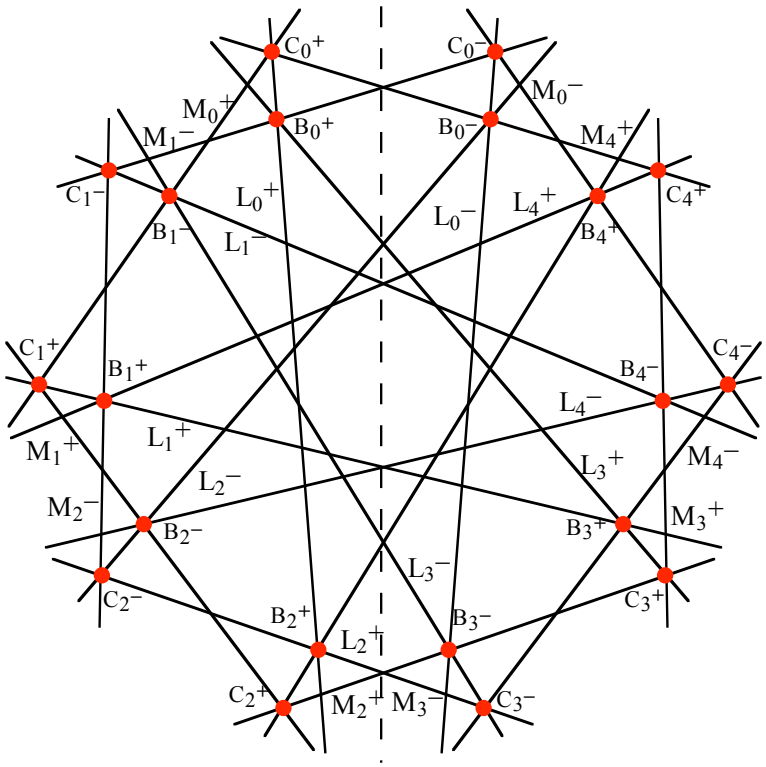

Figure 2.8.4. A dihedral astral configuration (20_3), with symmetry group d_5. The labeling illustrates the description given in the text. The configuration has symbol 5#(2,1; 1; 0.6).

As in the case of chiral astral configurations, the construction leads to a quadratic equation for λ. Again, the various possibilities and properties encountered with the chiral astral configurations (n_3) are largely present. In particular, depending on the values of the parameters m, b, c, d, μ of the configuration m#(b, c; d; μ), there can be two, one, or no real solutions. Moreover, for suitable values of these parameters the resulting construction leads to superfigurations. However, there has been very little done on a systematic investigation of the DD configurations. Several additional examples of such configurations and a case of superfiguration are shown in Figures 2.8.5 and 2.8.6.

There is no information available concerning the range of values of d for given m, b, c and μ, or concerning the possible values of λ for given m, b, c, d, μ. Equally missing is any knowledge concerning duality, polarity, selfduality and selfpolarity of DD configurations.

As with chiral astral configurations, the reduced Levi diagrams for dihedral astral 3-configurations are very simple and straightforward. This is illustrated in Figure 2.8.7, which demonstrates the mutual reinforcing of the notation introduced above, and the graphs.

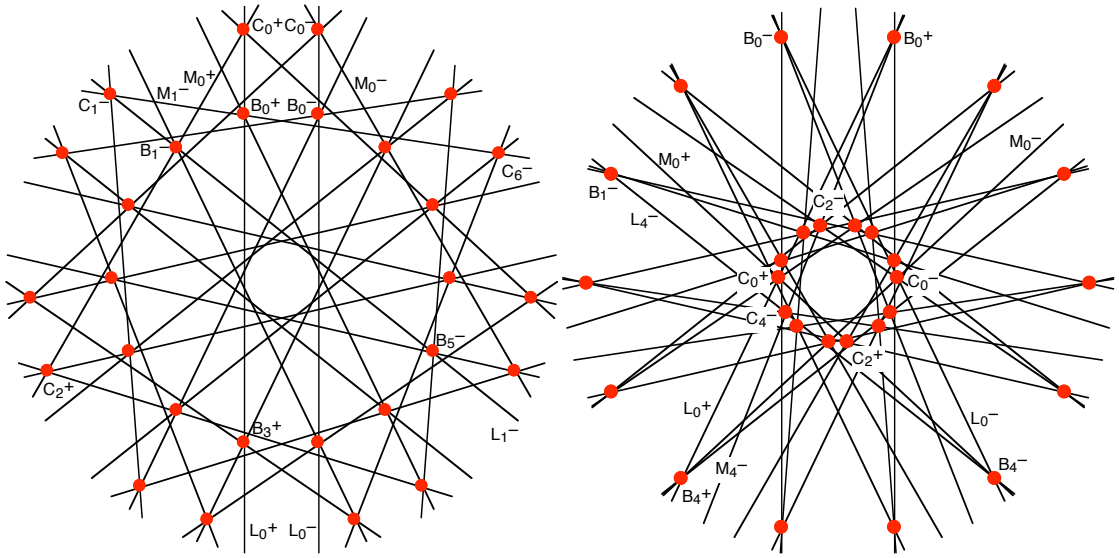

(a) (b)

Figure 2.8.5. Two dihedral astral configurations (28_3). To reduce clutter, only the labels needed for the determination of the symbol are shown. (a) 7#(3,2;1;1.0) (b) 7#(3,2;4;1.0).

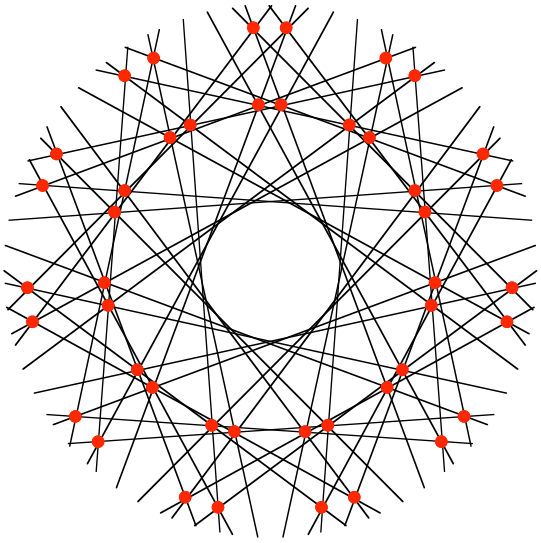

Figure 2.8.6. For a value of μ close to 0.5, the construction of the configuration 7#(4,3;1;μ) leads to a superfiguration: there are unintended incidences, yielding points on four lines and lines through four points.

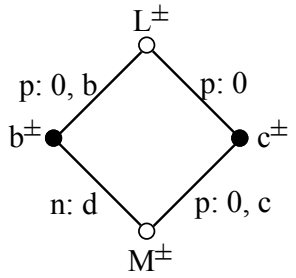

Symmetry group d_{2m}

Figure 2.8.7. The reduced Levi graph of the dihedral astral configuration m#(b,c;d;μ). The construction of the graph follows the method given in Section 1.6, based on the labeling of these configurations described above and illustrated in Figures 2.8.4 and 2.8.5. If the inclusion of the parameter in the graph is desirable, it can be attached to the 0 on the edge going from $L^{\pm}$ to $c^{\pm}$.

First examples of the third variety of dihedral astral 3-configurations were discovered only last year, and appear in the paper [B11] by L. W. **B**erman and J. **B**okowski.[1] We shall designate all configurations of this variety by BB with appropriate parameters attached. Any BB configuration (n_3) has $n = 3m$ for an integer $m \geq 5$. The configuration depends on two other parameters which we call s and t. The meaning of these parameters will be explained as we describe the construction of the configuration BB(m; s, t). We shall illustrate the construction in the case of BB(5; 2, 2), see Figure 2.8.8, but use general terms in the explanation of the steps.

The first step (Figure 2.8.8a) is the construction of a regular m-gon P, and selecting the midpoints of its sides; these midpoints are m of the points of the configuration, and the lines L_j determined by the sides of the m-gon are m of the lines. (The vertices of the m-gon play no added role in the construction, and are not marked in Figure 2.8.8.)

The second step (Figure 2.8.8b) is the selection of a chord of P of span s, and constructing the circumcircle C of the triangle determined by the endpoints of the chord and the center of P. The parameter s needs to be in the range $2 \leq s < m/2$.

---

[1] I had the privilege of receiving a preprint of this paper from the authors.

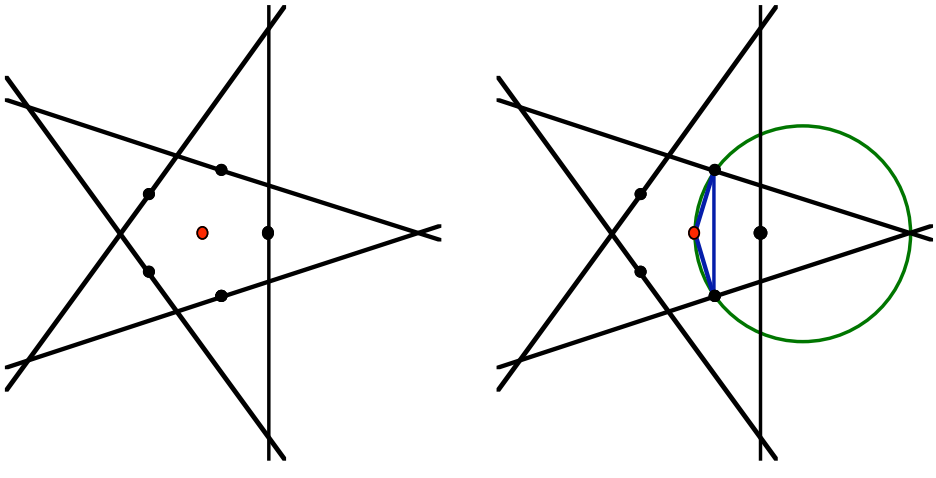

(a)

(b)

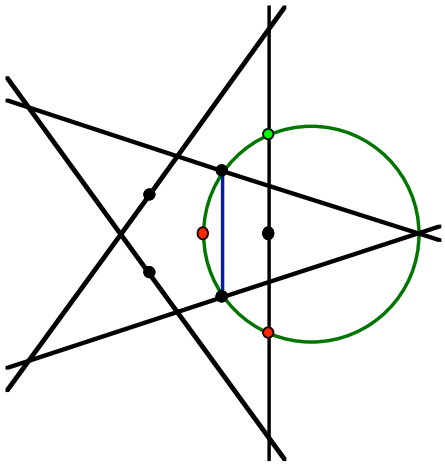

(c)

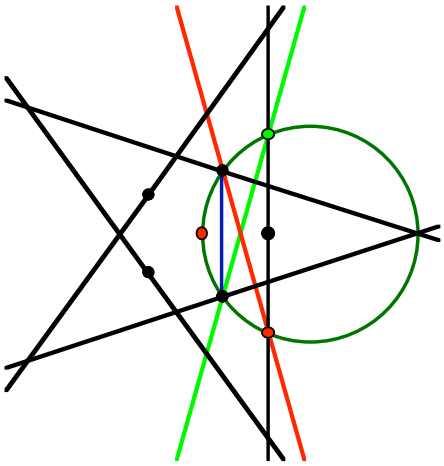

(d)

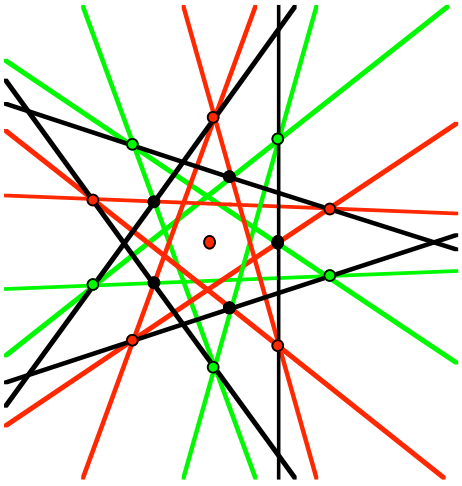

(e)

Figure 2.8.8. The steps in the construction of the configuration BB(5;2,2).

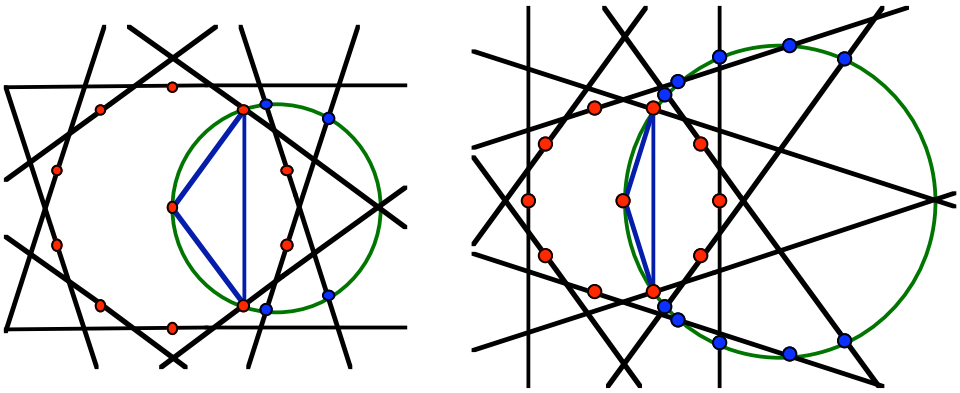

(a) (b)

Figure 2.8.9. Illustration of the possibilities in the third step of constructing configurations BB(10; s, t). In part (a) $s = 3$ and t is either 2 or 3. In part (b) $s = 4$ and $2 \le t \le 6$.

The third step (Figure 2.8.8c) consists in determining the intersections of the circle C with the lines L_j constructed in the first step. These intersection points always came in symmetric pairs. In case $m = 5$ (hence $s = 2$) there is only one such pair; the examples in Figure 2.8.9 show other possibilities. There are always at least $s–1$ pairs, and no more than $2s – 3$. The precise number depends on m and s in a manner that has not been explicitly determined.

In the fourth step (Figure 2.8.8d) a selected pair of these intersection points is connected by lines with the endpoints of the chord of span s with which we started in the second step. (To avoid clutter, in Figure 2.8.8d each point of the pair is connected with only one endpoint of the chord.) The parameter t is the label that can be given to the pairs, counting from the endpoints of the chord.

The fifth and final step (Figure 2.8.8e) consists in creating the images of the chosen pair of points and the lines generated in the previous step, by rotations about the center of the polygon P through all the multiples of $2\pi/m$.

Some remarks about the BB configurations. First, just as in the case of the DD configurations (and the chiral astral ones), in some instances the construction does not yield the expected configuration; instead a superfiguration is obtained. This is illustrated

in Figure 2.8.10. Also, the precise relations between the parameters of a BB configuration have not been determined so far. This is illustrated in Table 2.8.1, which shows the (experimentally determined) maximal value of t for given m and s.

m \ s	2	3	4	5	6	7	8	9	10	11	12	13	14	15	16	17	18
5	2																
6	2																
7	2	3															
8	2	3															
9	2	3	6														
10	2	3	6														
11	2	3	6	7													
12	2	3	4*	7													
13	2	3	4	7	10												
14	2	3	4	7	8												
15	2	3	4	7	8	11											
16	2	3	4	7	8	11											
17	2	3	4	7	8	11	12										
18	2	3	4	7	8	9	12										
19	2	3	4	7	8	9	12	15									
20	2	3	4	7	8	9	12	13									
21	2	3	4	7	8	9	12	13	16								
22	2	3	4	7	8	9	12	13	16								
23	2	3	4	7	8	9	12	13	16	19							
24	2	3	4	7	8	9	10*	13	14	17							
25	2	3	4	7	8	9	10	13	14	17	20						
26	2	3	4	7	8	9	10	13	14	17	20						
27	2	3	4	7	8	9	10	13	14	17	18	21					
28	2	3	4	7	8	9	10	13	14	17	18	21					
29	2	3	4	7	8	9	10	13	14	15	18	21	22				
30	2	3	4	7	8	9	10	13	14	15	18	19	22				
31	2	3	4	7	8	9	10	13	14	15	18	19	22	25			
32	2	3	4	7	8	9	10	13	14	15	18	19	22	25			
33	2	3	4	7	8	9	10	13	14	15	18	19	22	23	28		
34	2	3	4	7	8	9	10	13	14	15	18	19	22	23	26		
35	2	3	4	7	8	9	10	13	14	15	18	19	22	23	26	29	
36	2	3	4	7	8	9	10	13	14	15	16*	19	20	23	26	29	
37	2	3	4	7	8	9	10	13	14	15	16	19	20	23	24	27	32

(*) One of the lines is tangent to the circle at its intersection with another line.

Table 2.8.1. The maximal values of t for given m and s in configurations BB(m; s,t).

The BB configurations considered in [B11] are presented in a way tyat is somewhat different from the one followed here. The Berman-Bokowski construction corresponds to the cases of even s only, and uses only that pair of intersection points which arises by the intersection of the circumcircle with the line parallel to the chord used to construct the circle. This pair is in general the "middle" pair in the third step of our construction.

Another phenomenon — again shared by other classes of configurations — is the possibility of the configuration being disconnected. This happens, for example with the configuration BB(16; 6,6) shown in Figure 2.8.11.

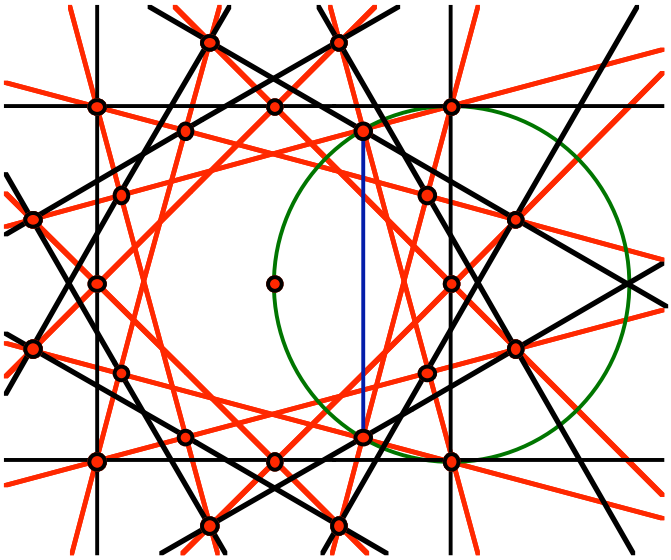

Figure 2.8.10. An example of a superfiguration arising in the construction of a BB type configuration with m = 12 and s = 4.

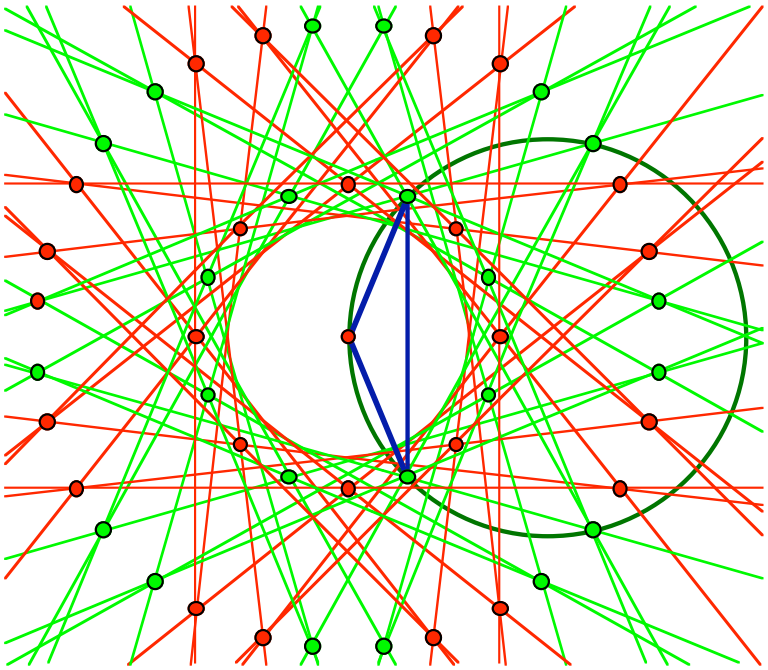

Figure 2.8.11. In the case of BB(16; 6, 6) the construction leads to a disconnected configuration. The two connected components are shown in different colors; each is BB(8; 3, 3).

While the construction procedure seems to be working in the examples given above, there is an obvious need for justification in the general case. It is, in fact, quite simple; we explain it for the configuration BB(m; s, t) by using the notation in the illustrative example shown in Figure 2.8.12, where $m = 9$, $s = 3$, and $t = 3$.

The chord of span s (used to generate the circumcircle K) spans an angle of $2\pi s/m$ at the center O of K. The line CB*, the legs of the isosceles triangle generated by the chord and O, and the segment OC are all well determined. Rotating this complex and the circle K about O through an angle of $2\pi s/m$ brings K to K*, CB* to C*B, and OC to OC*. The five angles denoted γ are all equal to each other because they are either basis angles of isosceles triangle, or spanned by congruent arcs of K. Hence the basis CC* of the isosceles triangle COC* encloses with the segment OC* the same angle γ as the line through C*B; hence that line passes through C, which justifies the construction.

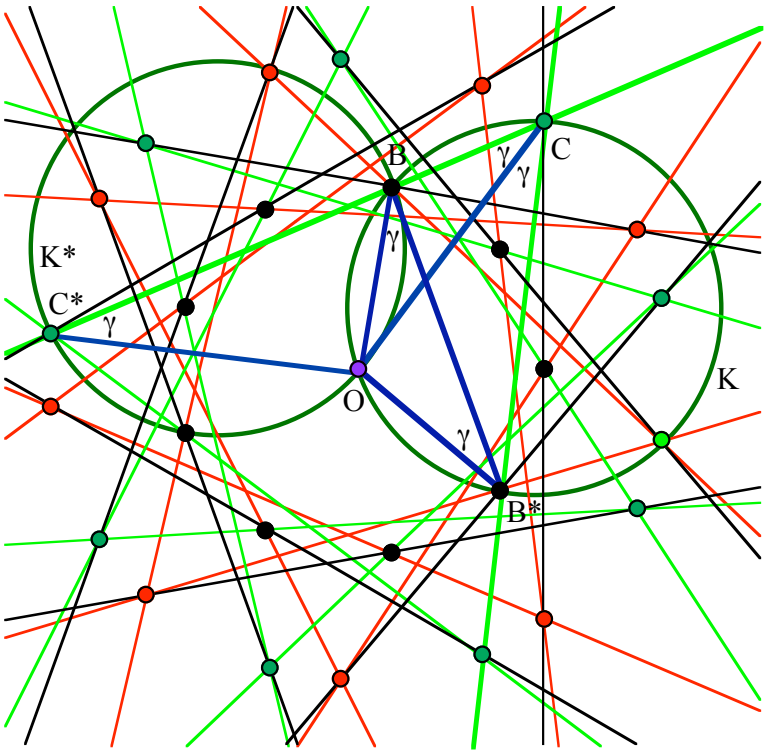

Figure 2.8.12. The validation of the construction of the BB configurations.

It should be noted that the procedure used to justify the construction dealt exclusively with the green lines. This leaves open the possibility to use a different value of t for the red lines. Naturally, the resulting configuration will not be astral.

Another point that needs to be made is the following. For each s, the set of values of t possible is a (non-strictly) decreasing function of m. The experimental results in Table 2.8.1 are a consequence of reasonably complicated trigonometric relations. The main problem in this context is to determine the maximal value of t possible in a BB(m; s,t) configuration. From numerical evidence (see Table 2.8.2) it seems that this t_{max} grows approximately as 7s/5 for sufficiently large m, although this appears a strange dependence.

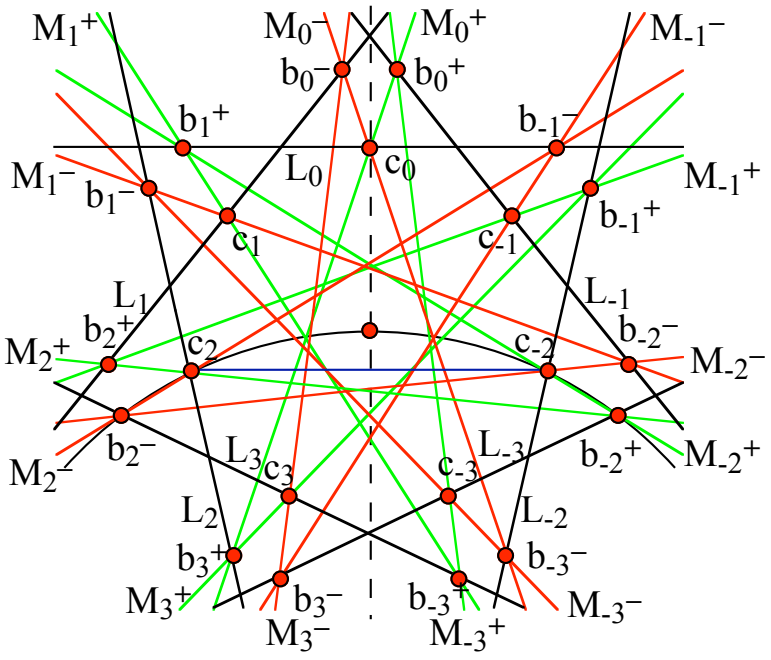

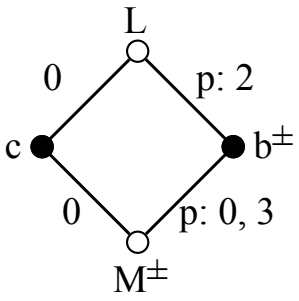

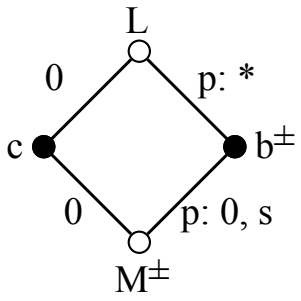

Figure 2.8.13. The labeling of BB configurations, and the resulting reduced Levi graphs. The graph at right corresponds to the general configuration BB(m; s, t); the asterisk indicates that no definite relation to the parameters has been found so far.

s	t_{max}	For m ≥
2	2	5
3	3	7
4	4	12
5	7	11
6	8	14
7	9	18
8	10	24
9	11	42
10	14	24
11	15	29
12	16	36
13	17	50
14	18	92
15	21	41
16	22	48
17	23	61
18	24	84
19	25	78
20	28	60

s	t_{max}	For m ≥
21	29	72
22	30	90
23	31	127
24	32	372
25	35	84
26	36	99
27	37	125
28	38	183
29	41	95
30	42	110
31	43	131
32	44	167
33	45	256
34	48	121
35	49	139
36	50	167
37	51	217
38	52	335
39	55	149
40	56	172

Table 2.8.2. The largest value t_{max} of t possible in configurations BB(m; s, t) for a given s and for all sufficiently large m.

Exercises and problems 2.8.

1. Determine what symbol could result for the configuration in Figure 2.8.4 if the role of B_0^+ and B_0^- were reversed, while still assuming conterclockwise orientation.

2. Determine what symbol could result for the configuration in Figure 2.8.4 if the role of the B-points and the C-points were reversed, while still assuming conterclockwise orientation.

3. Verify the assignment of symbols to the configurations in Figure 2.8.5.

4. Formulate a general criterion for the configuration BB(m; s,t) to be disconnected.

5. Draw all the different configurations BB(11; 5,t).

6. How many different configurations 4#(b, c; d; 0.3) are there?

7. Find some restrictions on the parameters of the DD and BB kinds of astral configurations.

8. Find disconnected configurations m#(b, c; d; μ).

9. Find a geometric construction for configurations m#(b, c; d; μ).

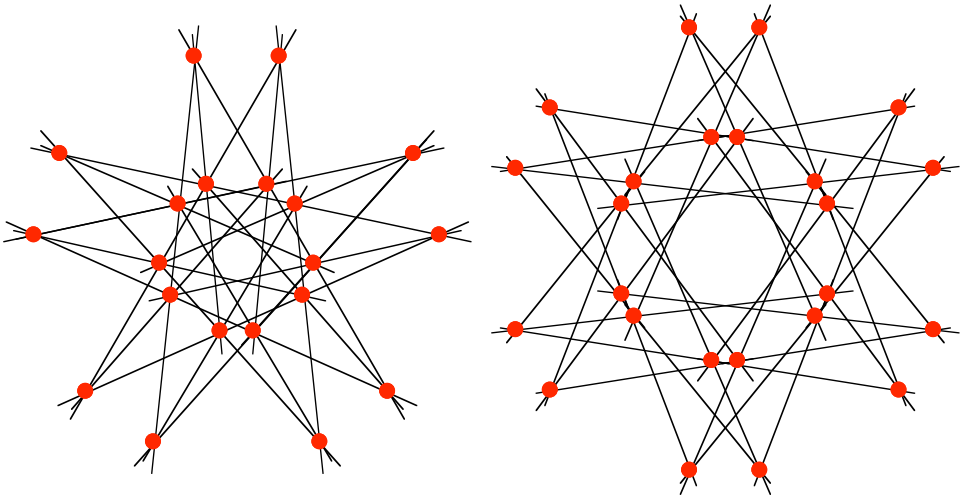

Figure 2.8.14. Two dihedral astral 3-configurations.

10. Find the symbols for the configurations in Figure 2.8.14.